Absolute Rate Constants for the Reactions of Cl Atoms with CH_3Br, CH_2Br_2, and $CHBr_3$

Kyriakos G. Kambanis, Yannis G. Lazarou, and Panos Papagiannakopoulos*

Department of Chemistry, University of Crete, Heraklion 714 09, Crete, Greece

Received: June 17, 1997[⊗]

The rate constants for the reactions of chlorine atoms with the complete series of the three bromomethanes CH_3Br (1), CH_2Br_2 (2), and $CHBr_3$ (3) were measured in a very low pressure reactor, employing a microwave discharge for the generation of Cl atoms with mass spectrometric detection of reactants and products. The experiments were performed in the temperature range 273−363 K and at total pressures ∼1 mTorr. The reactions proceed via hydrogen atom transfer leading to HCl product and the corresponding bromomethyl radicals. Their rate constant expressions are (in cm^3 $molecule^{-1}$ s^{-1}): $k_1 = (1.66 \pm 0.14) \times 10^{-11} \exp(-1072 \pm 46/T)$, $k_2 = (0.84 \pm 0.15) \times 10^{-11} \exp(-911 \pm 101/T)$, and $k_3 = (0.43 \pm 0.11) \times 10^{-11} \exp(-809 \pm 142/T)$. The activation energy of the reaction decreases with additional bromine substitution, which is attributed to the gradual weakening of the corresponding C−H bond strength. Ab initio theoretical calculations performed at the MP2/6-31++G(2d,2p) level of theory suggest C−H bond strengths for CH_3Br, CH_2Br_2, and $CHBr_3$ of 416.58, 407.03, and 396.60 kJ mol^{-1}, respectively.

Introduction

Bromine atoms are considered very effective in consuming stratospheric ozone;[1,2] therefore, the concentrations and chemical transformations of their atmospheric precursors have to be properly evaluated. Although biogenic processes release bromine containing organic compounds into the atmosphere, man-made contributions are suspected to contibute significantly, as several bromocompounds (CF_3Br, CF_2Br_2, CH_3Br) have found a variety of applications (fire extinguishers, pesticides, fumigants). The most abundant gas-phase bromocompound is CH_3Br, which has natural as well as anthropogenic sources,[1,3] followed by CH_2Br_2 and $CHBr_3$,[4] which are biogenic in origin. The atmospheric lifetime of the hydrogen-containing bromocompounds CH_3Br and CH_2Br_2 is primarily determined by degradation processes at tropospheric heights, mostly by their reactions with OH radicals. In the case of $CHBr_3$, which absorbs at the UV-A region of solar spectrum, rapid tropospheric photolysis may constitute its major removal pathway. However, at stratospheric heights, photolysis becomes the dominant degradation process of bromocompounds, leading to production of bromine atoms.

Chlorine atoms are also important stratospheric species, and they participate extensively in ozone destruction cycles. Their tropospheric significance is considered to be low,[5] although it has been proposed that they attain significant concentrations in coastal areas, generated from heterogeneous processes on sea-salt aerosols.[6,7] The gas-phase reactions of chlorine atoms are often used as a probe of the reactivity of several atmospheric species and the facile generation of the corresponding free radicals via hydrogen atom abstraction.

The reactions of Cl atoms with CH_3Br and CH_2Br_2 have been studied by several investigators,[8−11] and the corresponding rate constants are shown in Table 1. However, the reaction of Cl with $CHBr_3$ has not been studied in the past. The present study attempts to extend the kinetic information to $CHBr_3$ and allows the examination of the bromomethanes reactivity as a function of bromine substitution in a more systematic way.

Experimental Section

The reactions were studied in a very low pressure reactor (VLPR),[12] employing a microwave discharge as a source of Cl atoms and mass spectrometric monitoring of reactants and products. The thermostated cylidrical reactor ($V_{cell} = 168$ cm^3) was internally coated by a thin film of Teflon (Du-Pont Teflon 120) to inhibit the recombination of Cl atoms and radicals on the reactor walls and had two capillary inlets for the admission of each reactant. The reaction mixture was escaping through a cyclic orifice (5 mm diameter) to the first stage of a differentially pumped chamber. Thus, an effusive molecular beam was formed, which was collimated by a conical skimmer and entered the second vacuum chamber. It was further modulated by a tuning fork chopper with a frequency of 200 Hz and was analyzed with a quadrupole mass spectrometer (BALZERS QMG 511, electron impact ion source). A lock-in amplifier (NF LI-570) was used to select and amplify the modulated component of the mass spectrometric signal. A microcomputer (DEC microPDP-11) was used to collect the output of the lock-in amplifier and control the operation of the mass spectrometer.

The flow rates (in molecule s^{-1}) of the reactants were determined from the pressure drop in their buffer volumes as they were flowing into the reactor through long capillary resistances. The escape rate constant $k_{esc,M}$ of several species out of the reactor was measured as a function of their molecular weight M using their mass spectrometric signal first-order decay after a fast halt of their flow. Thus, $k_{esc,M}$ was given by the expression $1.86\ (T/M)^{1/2}$ (in s^{-1}), where T is the reactor temperature. The total pressure inside the reactor was calculated to be in the range 0.6−1.5 mTorr, and the partial pressure of

TABLE 1: Rate Constants for the Reactions of Cl Atoms with CH_3Br, CH_2Br_2, and $CHBr_3$

$10^{13}k_{298}$	$10^{11}A$	E_a/R	T range	ref
		CH_3Br		
5.53 ± 1.7	3.16 ± 0.63	1205 ± 69	273−368	8
4.16 ± 0.14	1.55 ± 0.18	1070 ± 50	222−393.5	9
4.45 ± 0.60	1.78 ± 0.25	1095 ± 60	231−296	10
4.40	$[3.2 \times 10^{-15}T^{1.26}$	$\exp(-670/T)]$	197−690	11
4.83 ± 0.12	1.66 ± 0.14	1072 ± 46	273−363	this work
		CH_2Br_2		
5.30 ± 1.6	9.53 ± 1.8	1547 ± 68	273−368	8
4.17 ± 0.08	0.64 ± 0.06	810 ± 50	222−394.5	9
4.42 ± 0.60	0.97 ± 0.15	906 ± 80	231−295	10
4.20 ± 0.21	0.84 ± 0.15	911 ± 101	273−363	this work
		$CHBr_3$		
3.04 ± 0.24	0.43 ± 0.11	809 ± 142	273−363	this work

[⊗] Abstract published in *Advance ACS Abstracts,* October 15, 1997.

S1089-5639(97)01967-1 CCC: $14.00

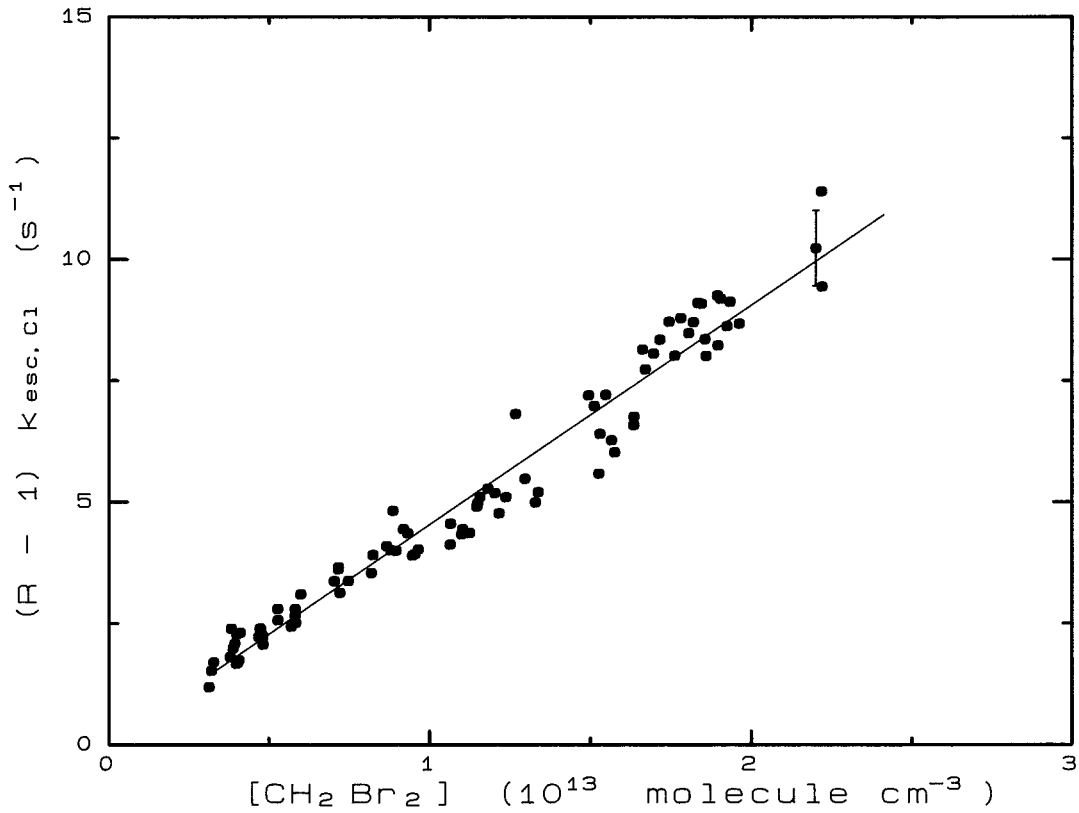

Figure 1. Plot of $(R - 1)k_{esc,Cl}$ vs $[CH_2Br_2]$ at $T = 303$ K. Error bar reflects the propagated error (2σ). Solid line is the linear least-squares fit to the data.

TABLE 2: Mass Spectra of CH_3Br, CH_2Br_2, and $CHBr_3$ at Two Electron Energies of 19 and 70 eV. Intensities Are Reported Relative to the Most Intense Peak Intensity

							CH_3Br							
mass	12	13	14	15	79	80	81	82	91	92	93	94	95	96
19 eV				99.7							3.5	100	3.5	98.3
70 eV	0.9	2.6	5.3	100	3.5	0.6	3.5	0.6	2.0	1.1	4.4	26.7	3.6	23.9
							CH_2Br_2							
mass	12	13	14	79	80	81	82	91	93	95	172	174	176	
19 eV			0.3						100	95.7	11.0	21.4	9.1	
70 eV	4.5	10.6	21.3	21.1	2.0	21.0	2.0	15.4	100	76.2	4.6	9.4	4.1	
							$CHBr_3$							
mass	12	13	14	79	80	81	82	91	92	93	94	171	173	175
19 eV				16.7	8.7	22.7	10.9					43.5	100	54.7
70 eV	17.8	44.8	3.2	85.2	9.4	90.7	9.1	100	44.0	97.5	48.7	18.6	43.8	21.7

helium was 0.5 mTorr. The residence time of a reactant in the reactor, given by the reciprocal of the sum of the rate constants of its loss processes (escape out of the reactor and chemical reactions), was calculated to be less than 0.2 s for Cl atoms, while for CH_3Br, CH_2Br_2, and $CHBr_3$ it was less than 0.3, 0.4, and 0.5 s, respectively.

Chlorine atoms were produced by a microwave discharge in a mixture of 5% Cl_2 in helium flowing through a quartz tube coated with a phosphoric−boric acid mixture in order to inhibit wall recombination of chlorine atoms. The conversion of Cl_2 to Cl atoms and HCl molecules (as a side product inside the discharge tube) was always complete as verified by the absence of *m*/*e* 70 (Cl_2^+) in the mass spectra. The electron energy of the ion source was set to 19 eV in order to suppress HCl fragmentation to *m*/*e* 35 (Cl^+) to negligible levels (∼0.3%) and thus eliminate the mass spectrometric interference of HCl in the measurements of Cl atoms. The stated purities of CH_3Br, CH_2Br_2, and $CHBr_3$ were >99.5%, >99%, and 97%, respectively, and they were frequently subjected to degassing procedures. The liquid reactants CH_2Br_2 and $CHBr_3$ were kept in darkened bulbs, above molecular sieves (0.4 nm) that absorb moisture and ethanol, used as a stabilizer for $CHBr_3$. Their purity was checked by mass spectrometry, and in all cases no decomposition products were found; however, two minor peaks at *m*/*e* 49 and 51 ($CH_2{}^{35}Cl^+$ and $CH_2{}^{37}Cl^+$, respectively) in the mass spectrum of CH_2Br_2 were attributed to CH_2ClBr impurity, which could not be removed. The mass spectra of CH_3Br, CH_2Br_2, and $CHBr_3$ at two electron energies (70 and 19 eV) are displayed in Table 2. The parent peak at *m*/*e* 94 was used to monitor CH_3Br, while the most intense peaks at *m*/*e* 93 (CH_2Br^+) and 173 ($CHBr_2^+$) were used to monitor CH_2Br_2 and $CHBr_3$, respectively; these peaks are not likely to have contributions from the mass spectrometric fragmentation of the corresponding free radical products of their reactions with Cl atoms. The correlation of the mass spectrometric peak intensity I_S of a species with its steady-state

TABLE 3: Rate Constants for the Reactions of Cl Atoms with CH_3Br, CH_2Br_2, and $CHBr_3$, Measured at Temperatures of 273, 303, 333, and 363 K

temp (K)	rate constant (10^{13} cm^3 molecule^{-1} s^{-1})	no. of points
	Reaction Cl + CH_3Br	
273	3.21 ± 0.30	17
303	4.83 ± 0.12	11
333	6.75 ± 0.63	15
363	8.62 ± 0.35	10
	Reaction Cl + CH_2Br_2	
273	2.91 ± 0.20	28
303	4.20 ± 0.21	70
333	5.59 ± 0.56	19
363	6.72 ± 0.34	48
	Reaction Cl + $CHBr_3$	
273	2.12 ± 0.25	15
303	3.04 ± 0.24	49
333	3.90 ± 0.54	14
363	4.56 ± 0.27	16

concentration [S] was determined by calibration plots of the expression

$$I_S = \alpha_S V_{cell} k_{esc,S}[S] \qquad \text{(I)}$$

where α_S is a characteristic mass spectrometric calibration factor. The mass spectrometric intensity measurements had a deviation of ±5% (2σ).

All bromomethanes were introduced into the reactor undiluted. The flow of chlorine atoms was always kept constant, by maintaining the Cl_2/He mixture in the buffer volume at a certain pressure, while the flow of bromomethanes to the reactor was controlled by varying the pressure in their buffer volumes accordingly.

Results

The mass spectrometric analysis of the reaction products for the three bromomethanes reveals an increase of the peak at *m*/*e* 36 that is attributed to HCl product. In the case of CH_3Br and CH_2Br_2, there was no evidence for the production of Br atoms (at *m*/*e* 79, 80) or BrCl molecules (at *m*/*e* 114, 116, 118), indicating that bromine substitution or abstraction pathways were not occurring. However, in the case of $CHBr_3$, small peaks at *m*/*e* 114, 116, and 118 were observed, while the intensity of the weak peak at *m*/*e* 114 ($^{79}Br^{35}Cl^+$) was ca. 4% of the intensity loss of Cl atoms when $CHBr_3$ was added. The calibration factor for the parent peak of BrCl at *m*/*e* 114 was measured to be 1.29 ± 0.09 times higher than that of Cl atoms at *m*/*e* 35 (vide infra); thus, a yield of ca. 3% is derived for the bromine abstraction pathway in the reaction of $CHBr_3$ with Cl. Since the yield of BrCl is small, the kinetic effects of its possible secondary reaction with Cl atoms were considered negligible. Moreover, in all three cases the HCl product yield was found always equal to the Cl atoms consumption, within an accuracy of 10%. Therefore, the dominant pathway for the three reactions is the abstraction of a hydrogen atom:

$$CH_3Br + Cl \rightarrow CH_2Br + HCl \qquad (1)$$

$$CH_2Br_2 + Cl \rightarrow CHBr_2 + HCl \qquad (2)$$

$$CHBr_3 + Cl \rightarrow CBr_3 + HCl \qquad (3)$$

In addition, there was no mass spectrometric evidence for radical recombination reactions either with Cl atoms or with themselves; therefore, the kinetic scheme is free from secondary reactions complications. The parallel reaction of Cl atoms with the CH_2ClBr impurity in CH_2Br_2 was ignored since its rate constant was reported to be 4.18×10^{-13} cm^3 molecule^{-1} s^{-1} [8]

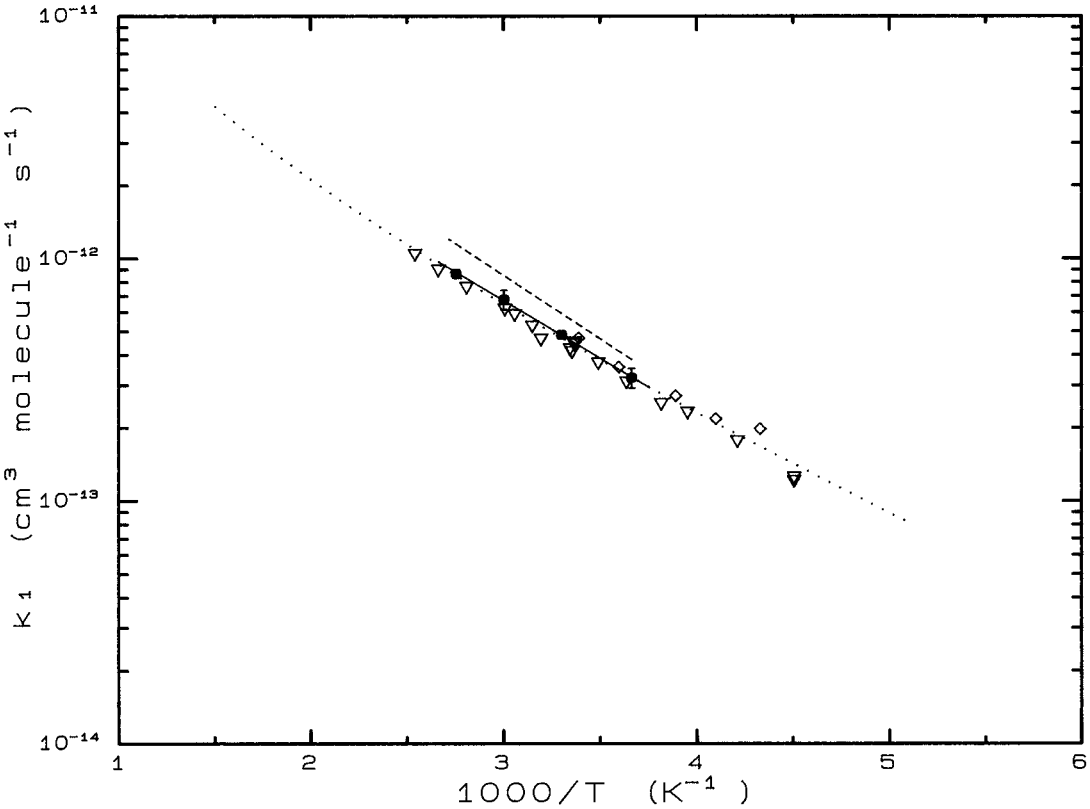

Figure 2. Arrhenius plot for reaction of Cl atoms with CH_3Br, filled circles; error bars reflect the propagated errors (2σ); solid line is the linear least-squares fit to the data. Dashed line drawn from rate parameters in ref 8; triangles and rhombohedrons represent the results of refs 9 and 10, respectively. Dotted line drawn from the non-Arrhenius expression in ref 11.

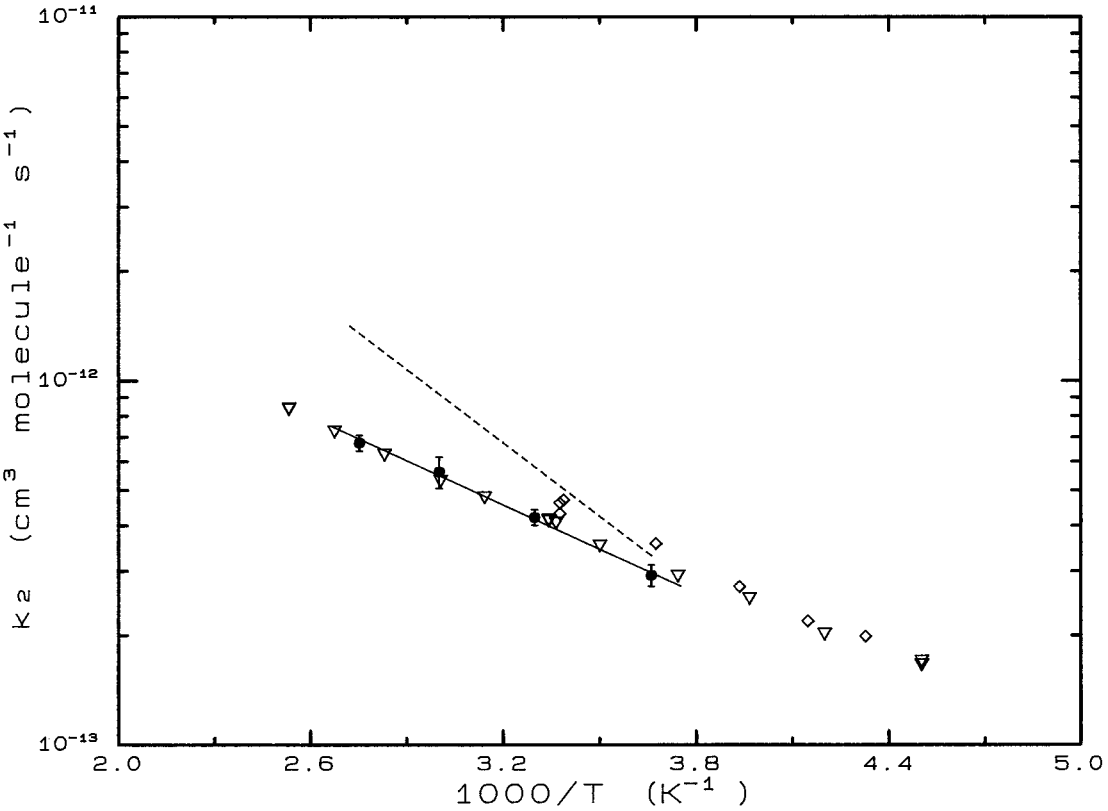

Figure 3. Arrhenius plot for reaction of Cl atoms with CH_2Br_2; filled circles; error bars reflect the propagated errors (2σ); solid line is the linear least-squares fit to the data. Dashed line drawn from rate parameters in ref 8; triangles and rhombohedrons represent the results of refs 9 and 10, respectively.

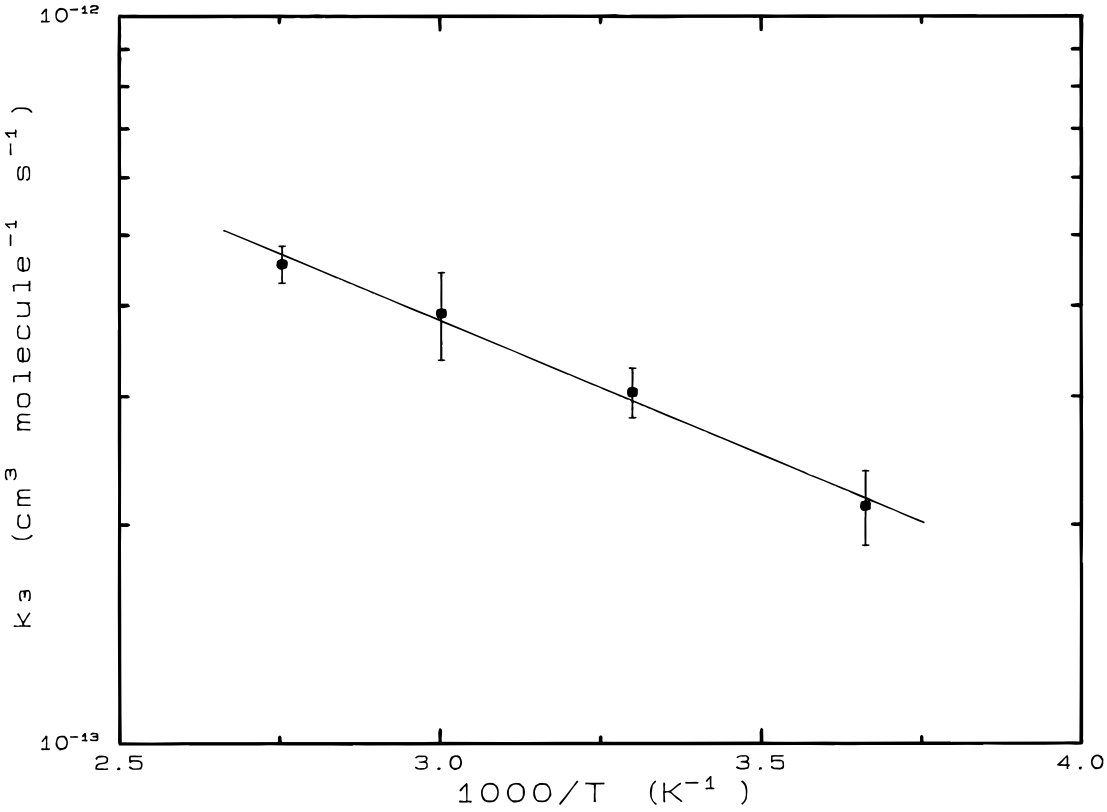

Figure 4. Arrhenius plot for reaction of Cl atoms with $CHBr_3$. Error bars reflect the propagated errors (2σ), solid line is the linear least-squares fit to the data.

(in the order of k_2) and its concentration is 100 times lower than that of CH_2Br_2.

Derivation of the Kinetic Equations. In the absence of any reaction, the flow of Cl atoms in the reactor must equal their escape rate out of the reactor; thus, a steady-state concentration of Cl atoms is maintained, expressed as

$$F_{Cl}/V_{cell} = k_{esc,Cl}[Cl]_o \qquad \text{(II)}$$

In the presence of a species RH capable of reacting with Cl atoms, the flow of Cl atoms in the reactor equals their escape rate plus their reaction rate k, expressed as

$$F_{Cl}/V_{cell} = k_{esc,Cl}[Cl]_r + k[Cl]_r[RH] \qquad (III)$$

where subscripts o and r refer to absence and presence of RH, respectively. Since the flow of chlorine atoms was always kept constant, application of the steady-state approximation for Cl atoms and reaction 1 leads to

$$[Cl]_o k_{esc,Cl} = [Cl]_r k_{esc,Cl} + k_1[Cl]_r[CH_3Br] \qquad (IV)$$

After minor rearrangement, and expressing the difference ($[Cl]_o - [Cl]_r$) as Δ[Cl], the above equation becomes

$$\Delta[Cl]\, k_{esc,Cl} = k_1[Cl]_r[CH_3Br] \qquad (V)$$

which is transformed into the final equation, considering the linear dependence of the mass spectrometric intensity on the steady-state concentration (expression I)

$$(R - 1)k_{esc,Cl} = k_1\,[CH_3Br] \qquad (VI)$$

where R denotes the mass spectrometric intensity ratio $I_{Cl,o}/I_{Cl,r}$.

Kinetic Results. The experimental runs for reaction 1 were performed by monitoring the drop in Cl atoms signal intensity as CH_3Br reactant was alternately added or withheld. The peak intensity at *m*/*e* 94 (CH_3Br^+) was simultaneously measured and was correlated with the steady-state concentration [CH_3Br] via the calibration plots. The experiments were performed at four temperatures of 273, 303, 333, and 363 K. Similar experimental procedures were performed for the corresponding reactions of CH_2Br_2 and $CHBr_3$. The steady-state Cl atoms concentrations ranged from 1.5×10^{11} molecules cm^{-3} to 5.5×10^{11} molecules cm^{-3}, while those of bromomethanes ranged from 1.0×10^{12} molecules cm^{-3} to 2.5×10^{13} molecules cm^{-3}. A typical plot of $(R - 1)k_{esc,Cl}$ vs [CH_2Br_2] at 303 K is shown in Figure 1. The slopes of the linear least-squares fits to the data provided the rate constants, and the results obtained for the three reactions are listed in Table 3. The corresponding Arrhenius plots in the temperature range 273−363 K are shown in Figures 2, 3, and 4, respectively, and the rate constants derived are (2σ uncertainties, in cm^3 $molecule^{-1}$ s^{-1})

$$k_1 = (1.66 \pm 0.14) \times 10^{-11} \exp(-1072 \pm 46/T)$$

$$k_2 = (0.84 \pm 0.15) \times 10^{-11} \exp(-911 \pm 101/T)$$

$$k_3 = (0.43 \pm 0.11) \times 10^{-11} \exp(-809 \pm 142/T)$$

Measurement of the Calibration Factor of BrCl at *m*/*e* 114. Separate experiments were performed in order to measure the mass spectrometric calibration factor of BrCl at *m*/*e* 114 relative to that of Cl atoms, at an electron energy of 19 eV, by using the fast reaction of Cl atoms with Br_2 molecules ($k_4 = (1.20 \pm 0.15) \times 10^{-10}$ cm^3 $molecule^{-1}$ s^{-1} at 298 K[13]):

$$Br_2 + Cl \rightarrow BrCl + Br \qquad (4)$$

A great excess of Br_2 was used in order to minimize the contribution of the slower secondary reaction ($k_5 = (1.45 \pm 0.20) \times 10^{-11}$ cm^3 $molecule^{-1}$ s^{-1} at 298 K[13]):

$$BrCl + Cl \rightarrow Cl_2 + Br \qquad (5)$$

TABLE 4: Optimized Structural Parameters,[a,b] Vibrational Frequencies,[a,c] and Zero-Point Energies (ZPE)[d] for CH_3, CH_3Br, CH_2Br, CH_2Br_2, $CHBr_2$, $CHBr_3$, and CBr_3

species	geometrical parameters	vibrational frequencies	ZPE
CH_3	C−H, 1.074	523.2, 1504.5,	72.86
	∠H−C−H, 120.00	1507.1, 3253.3,	
	τ H−C(−H)−H, 180.00	3437.9, 3460.9	
CH_3Br	C−Br, 1.992; C−H, 1.083	586.1, 972.7,	88.60
	∠H−C−H, 111.87	973.5, 1359.4,	
	∠H−C−Br, 106.95	1483.1, 1484.3,	
	τ H−C(−Br)−H, 120.00	3173.1, 3296.9,	
		3314.5	
CH_2Br	C−Br, 1.889; C−H, 1.069	133.8, 677.0,	53.97
	∠H−C−H, 125.40	969.9, 1462.3,	
	∠H−C−Br, 117.31	3356.3, 3538.4	
	τ H−C(−Br)−H, 180.00		
CH_2Br_2	C−Br, 1.969; C−H, 1.080	168.0, 569.4,	66.97
	∠H−C−H, 114.04	630.5, 805.1,	
	∠H−C−Br, 107.83	1149.5, 1251.0,	
	∠Br−C−Br, 111.55	1428.1, 3234.1,	
	τ H−C(−Br)−H, 123.57	3344.0	
	τ H−C(−Br)−Br, 118.21		
$CHBr_2$	C−Br, 1.883; C−H, 1.070	186.6, 392.2,	35.59
	∠H−C−Br, 117.36	610.2, 780.4,	
	∠Br−C−Br, 119.32	1256.2, 3459.3	
	τ H−C(−Br)−Br, 152.17		
$CHBr_3$	C−Br, 1.960; C−H, 1.079	151.2, 151.7,	43.03
	∠H−C−Br, 107.90	215.6, 519.2,	
	∠Br−C−Br, 111.00	655.8, 658.3,	
	τ H−C(−Br)−Br, 118.03	1201.1, 1202.0	
	τ Br−C(−Br)−Br, 123.94	3329.1	
CBr_3	C−Br, 1.884	164.3, 164.8,	13.07
	∠Br−C−Br, 118.10	183.0, 302.3,	
	τ Br−C(−Br)−Br, 152.95	818.3, 821.7	

[a] At the 3-21++G(2d,2p) level of theory, including second-order Møller−Plesset perturbation (MP2, frozen core) for CH_3Br, CH_2Br_2, and $CHBr_3$. [b] Bond lengths in angstroms, bond (∠) and dihedral angles (τ) in degrees. [c] Scaled by 0.89; in cm^{-1}. [d] Using vibrational frequencies scaled by 0.89; in kJ mol^{-1}.

Application of the steady-state approximation for Cl atoms and BrCl molecules leads to

$$\Delta[Cl]k_{esc,Cl} = [BrCl]k_{esc,BrCl} \qquad (VII)$$

Using expression I, the above equation becomes

$$\Delta I_{Cl}\, \alpha_{BrCl} = I_{BrCl}\, \alpha_{Cl}$$

Thus, the ratio $\alpha_{BrCl}/\alpha_{Cl}$ can be determined by the ratio of the BrCl product intensity at *m*/*e* 114 to the corresponding drop in Cl atoms intensity at *m*/*e* 35. An average of five measurements gave a $\alpha_{BrCl}/\alpha_{Cl}$ ratio of 1.29 ± 0.09. In addition, the mass spectrum of BrCl at an electron energy of 19 eV was determined to be (relative intensities in parentheses): 35 (3.9), 37 (1.2), 79 (12.1), 81 (12.1), 114 (82.7), 116 (100), and 118 (22.4).

Discussion

The rate parameters of the reactions of Cl atoms with CH_3Br and CH_2Br_2 are in very good agreement with the results of three recent experimental studies,[9−11] and in rather poor agreement (especially for CH_2Br_2) with an earlier study,[8] as can be seen in Table 1. The results show a systematic trend toward a decrease of the activation energy, the preexponential *A* factor, and the rate constant as a function of increasing degree of bromine substitution in bromomethanes. A similar decline of the *A* factor and the activation energy is observed for the corresponding OH radical reactions, although the rate constants show an inverse trend.[14] The decrease of the preexponential factors as the number of bromine atoms is increasing can be explained by the smaller entropic differences between reactants

TABLE 5: Total Electronic Energies (E_0) and Total Enthalpies at 0.0 and 298.15 K (H_0, H_{298}) of All Species, Calculated at MP2/3-21++G(2d,2p) and MP2/6-31++G(2d,2p) Levels of Theory (in hartrees; 1 hartree = 2625.5 kJ mol^{-1})

	total energy					
	MP2/3-21++G(2d,2p)			MP2/6-31++G(2d,2p)		
species	E_0	H_0	H_{298}	E_0	H_0	H_{298}
H	−0.497 800	−0.497 800	−0.495 440	−0.498 801	−0.498 801	−0.496 441
Br	−2560.500 308	−2560.500 308	−2560.497 948	−2570.138 216	−2570.138 216	−2570.135 856
CH_3	−39.474 648	−39.446 897	−39.442 850	−39.708 159	−39.680 408	−39.676 361
CH_3Br	−2600.085 232	−2600.051 486	−2600.047 341	−2609.969 580	−2609.935 834	−2609.931 689
CH_2Br	−2599.416 225	−2599.395 670	−2599.390 963	−2609.301 844	−2609.281 290	−2699.276 582
CH_2Br_2	−5160.026 944	−5160.001 437	−5159.996 439	−5179.561 064	−5179.535 556	−5179.530 559
$CHBr_2$	−5159.358 743	−5159.345 187	−5159.340 101	−5178.897 731	−5178.884 176	−5178.879 089
$CHBr_3$	−7719.967 449	−7719.951 057	−7719.944 721	−7749.154 037	−7749.137 646	−7749.131 309
CBr_3	−7719.301 906	−7719.296 929	−7719.290 569	−7748.495 150	−7748.490 173	−7748.483 813

and transition states, mainly determined by their external rotational degrees of freedom. The concurrent decrease of the activation energy most possibly reflects the weakening of the C−H bond strengths. The ratios k_{Cl}/k_{OH} of their rate constants with Cl atoms to those with OH radicals show a decline from more than an order of magnitude for CH_3Br to a factor of almost 2 for $CHBr_3$. Thus, as the number of bromine atoms increases, the rate constants are becoming less sensitive to the nature of the attacking radical species. However, these correlations should also consider the possibility of intermediate adducts formation between bromomethanes and the incoming Cl atom or OH radical. The formation of weakly bound adducts between CH_3Br molecule and Cl atom has been proposed on the basis of experimental results[11] and is also supported by ab initio calculations.[11,15] The experimental CH_3Br-Cl bond strength at 298 K was reported to be 24.5 kJ mol^{-1},[11] in accordance with our ab initio estimation of 28.49 kJ mol^{-1}.[15] Since the CH_3Br-Cl bond is very weak, collisional stabilization of the CH_3BrCl adduct is likely to be an inefficient process, with negligible effects on the kinetics of the reaction of Cl atoms with CH_3Br. Indeed, this reaction has been performed at total pressures ranging from 1 mTorr to almost 1 atm, with almost no pressure effect on the activation energy.[9,10] However, in the reaction of Cl atoms with CH_3I, an increase of the apparent activation energy with pressure was observed,[11,16] and this was attributed to collisional stabilization of the CH_3ICl adduct.[16] The CH_3I-Cl bond strength was calculated by ab initio theoretical methods to be 52.41 kJ mol^{-1},[17] almost twice the corresponding CH_3Br-Cl bond strength. Thus, in the CH_3BrCl adduct, the pathway of dissociation back to its constituents is much faster than its forward pathway of decomposition to CH_2Br and HCl products, considering that a higher energy barrier must be surmounted in the forward direction and significant molecular rearrangements must take place. Furthermore, due to the very low energy barrier in the backward direction, any effect of collisional stabilization of the adduct should be canceled out by its collisional energization; thus, the rate back to reactants should be independent of pressure. As a result, the kinetics of the overall reaction are not affected by the total pressure.

To examine the effects of bromine substitution on the strength of the C−H and C−Br bonds, we have performed ab initio theoretical calculations, using the GAMESS computational programs package.[18] Restricted Hartree−Fock (RHF) and unrestricted Hartree−Fock (UHF) wave functions were used for closed and open shell species, respectively. The 3-21G and 6-31G basis sets were employed, augmented by adding two sets of polarization functions and diffuse functions to all atoms. Second-order Møller−Plesset perturbation theory (MP2, frozen core) was used in order to take correlation effects into account. No symmetry constraints were imposed in all calculations. Geometry optimizations and vibrational frequency calculations of bromomethanes were performed at the MP2/RHF/3-21++G-(2d,2p) level of theory, while those of the radical species were performed at the UHF/3-21++G(2d,2p) level. The calculated vibrational frequencies were scaled down by the factor 0.89 in order to compensate for anharmonicity effects.[19] Structural parameters, vibrational frequencies, and zero-point energies of CH_3, CH_3Br, CH_2Br, CH_2Br_2, $CHBr_2$, $CHBr_3$, and CBr_3 are shown in Table 4. Single-point energy calculations of all species at the MP2/3-21++G(2d,2p) and MP2/6-31++G(2d,2p) levels of theory were performed using their optimized geometries. The total enthalpies and the C−H and C−Br bond strengths were calculated at two temperatures (0.0 and 298.15 K), assuming the rigid-rotor and harmonic oscillator approximations, and the results are shown in Tables 5 and 6, respectively. The theoretical results indicate a reduction in C−H bond strength with increasing bromine substitution, especially with the larger and more reliable basis set of 6-31++G(2d,2p). Thus, at standard temperature (298.15 K), the C−H bond strengths of CH_3Br, CH_2Br_2, and $CHBr_3$ were calculated to be 416.58, 407.03, and 396.60 kJ mol^{-1}, respectively. Considering the currently accepted heats of formation of bromomethanes and bromomethyl radicals,[20] the C−H bond strengths derived (420.5 ± 8.4, 416.7 ± 12, and 392.5 ± 12 kJ mol^{-1}, respectively) are in very good agreement with the theoretical estimates of the present study.

TABLE 6: Ab Initio C−H and C−Br Bond Dissociation Energies (in kJ mol^{-1}) for CH_3Br, CH_2Br_2, and $CHBr_3$, Calculated at 0.0 and 298.15 K at the MP2/3-21++G(2d,2p) and MP2/6-31++G(2d,2p) Levels of Theory. The Experimental Values Are Calculated from Thermochemical Data Available (in ref 20)

	dissociation energy				
	MP2/3-21++G(2d,2p)		MP2/6-31++G(2d,2p)		exptl
bond	0 K	298.15 K	0 K	298.15 K	298 K
BrH_2C-H	414.870	422.543	408.903	416.576	420.5 ± 8.4
Br_2HC-H	416.007	422.438	400.598	407.028	416.7 ± 12
Br_3C-H	410.440	416.699	390.336	396.595	392.5 ± 12
H_3C-Br	273.791	279.728	307.734	313.672	293.4 ± 0.8
BrH_2C-Br	276.880	282.315	304.690	310.125	289.7 ± 12
Br_2HC-Br	277.152	280.069	302.598	305.514	274.6 ± 12

The calculated C−Br bond strengths at the MP2/6-31++G-(2d,2p) level of theory show a similar effect of bond weakening upon increasing bromine substititution, unlike the results at the lower MP2/3-21++G(2d,2p) level, which show no particular trend. Using the higher level of MP2/6-31++G(2d,2p), the computed C−Br bond strengths at 298.15 K were calculated to be 313.67, 310.13, and 305.51 kJ mol^{-1} for CH_3Br, CH_2Br_2, and $CHBr_3$, respectively. In comparison, the corresponding C−Br bond strengths, derived from thermochemical data[20] (293.4 ± 0.8, 289.7 ± 12, and 274.6 ± 12 kJ mol^{-1}, respectively) are ∼20 kJ mol^{-1} lower. However, the relatively small deviation of the theoretical predictions from the experimentally determined values should be considered acceptable

within the chemical accuracy of ab initio molecular mechanics calculations at these levels of theory. In conclusion, the theoretical results of this study are providing strong support for the currently available thermochemical data of bromine-containing compounds.

The tropospheric degradation of CH_3Br and CH_2Br_2 via their reactions with Cl atoms may contribute significantly only at the marine boundary layer, considering the possibility of elevated Cl atom concentrations near the sea surface, as it has already been discussed.[9] In the case of $CHBr_3$, its reaction with the more abundant OH radicals is only a factor of 2 slower than with Cl atoms,[14] and its photolysis is probably an important tropospheric loss process. Therefore, the contibution of its reaction with Cl atoms to the tropospheric chemistry of $CHBr_3$ is expected to be small, since the competing pathways (reaction with OH radicals, photolysis) are much more effective.

References and Notes

(1) World Meteorological Organization (WMO), Scientific Assessment of Ozone Depletion, 1994. Report No. 37; WMO: Geneva, 1995.

(2) Tang, T.; McConnell, J. C. *Geophys. Res. Lett.* **1996**, *23*, 2633−2636.

(3) Butler, J. H. *Geophys. Res. Lett.* **1994**, *21*, 185−188.

(4) Schall C.; Heumann, K. G. *Fresenius J. Anal. Chem.* **1993**, *346*, 717−722.

(5) Rudolph, J.; Koppmann, R.; Plass-Dülmer, C. *Atmos. Environ.* **1996**, *30*, 1887−1894.

(6) Finlayson-Pitts, B. J.; Ezell, M. J.; Pitts, J. N., Jr. *Nature*, **1989**, *337*, 241−244.

(7) Keene, W. C.; Jacob, D. J.; Fan, S.-M. *Atmos. Environ.* **1996**, *30*, i−iii.

(8) Tschuikow-Roux, E.; Faraji, F.; Paddison, S.; Niedzielski, J.; Miyokawa, K. *J. Phys. Chem.* **1988**, *92*, 1488−1495.

(9) Gierczak, T.; Goldfarb, L.; Sueper, D.; Ravishankara, A. R. *Int. J. Chem. Kinet.* **1994**, *26*, 719−728.

(10) Orlando, J. J.; Tyndall, G. S.; Wallington, T. J.; Dill, M. *Int. J. Chem. Kinet.* **1996**, *28*, 433−442.

(11) Piety, C. A.; Nicovich, J. M.; Ayhens, Y. V.; Estupinan, E. G.; Soller, R.; McKee, M. L.; Wine, P. H. *Proceedings of the 14th International Symposium on Gas Kinetics*; University of Leeds: Leeds, U.K., 1996.

(12) Lazarou, Y. G.; Michael, C.; Papagiannakopoulos, P. *J. Phys. Chem.* **1992**, *96*, 1705−1708.

(13) Clyne, M. A. A.; Cruse, H. W. *J. Chem. Soc., Faraday Trans. 2* **1972**, 68, 1377−1387.

(14) DeMore, W. B. *J. Phys. Chem.* **1996**, *100*, 5813−5820.

(15) Lazarou, Y. G.; Kambanis, K. G.; Papagiannakopoulos, P. To be submitted to *J. Phys. Chem.*

(16) Kambanis, K. G.; Lazarou, Y. G.; Papagiannakopoulos, P. *Chem. Phys. Lett.* **1997**, *268*, 498−504.

(17) Lazarou, Y. G.; Kambanis, K. G.; Papagiannakopoulos, P. *Chem. Phys. Lett.* **1997**, *271*, 280−286.

(18) Schmidt, M. W., Baldridge, K. K.; Boatz, J. A.; Elbert, S. T.; Gordon, M. S.; Jensen, J. H.; Koseki, S.; Matsunaga, N.; Nguyen, K. A.; Su, S. J.; Windus, T. L.; Dupuis, M; Montgomery, J. A. *J. Comput. Chem.* **1993**, *14*, 1347−1363.

(19) Hehre, W. J.; Radom, L.; Schleyer, P.v. R.; Pople, J. A. *Ab-initio Molecular Orbital Theory*; Wiley-Interscience: New York, 1986.

(20) DeMore, W. B.; Sander, S. P.; Golden, D. M.; Hampson, R. F.; Kurylo, M. J.; Howard, C. J.; Ravishankara, A. R.; Kolb, C. E.; Molina, M. J. Chemical Kinetics and Photochemical Data for Use in Stratospheric Modelling. JPL Publication *94−26*; JPL: Pasadena, CA, 1994.